medical sciences

MDPI

Article

Matrix Gla Protein in Patients with Colorectal Cancer

Ivna Olić [1,2], Ivan Maleš [3,4], Roko Šantić [5,6], Piero Marin Živković [1,5], Daniela Šupe Domić [7,8], Marko Kumrić [5,6] and Joško Božić [5,6,*]

1 Department of Gastroenterology, University Hospital of Split, Spinčićeva 1, 21000 Split, Croatia; ivna1211@gmail.com (I.O.); pzivkovic@kbsplit.hr (P.M.Ž.)
2 Doctoral Study Program Evidence-Based Medicine, University of Split School of Medicine, Šoltanska 2A, 21000 Split, Croatia
3 Department of Abdominal Surgery, University Hospital of Split, Spinčićeva 1, 21000 Split, Croatia; ivmales@kbsplit.hr
4 Department of Surgery, University of Split School of Medicine, Šoltanska 2A, 21000 Split, Croatia
5 Department of Pathophysiology, University of Split School of Medicine, Šoltanska 2A, 21000 Split, Croatia; roko.santic@mefst.hr (R.Š.); marko.kumric@mefst.hr (M.K.)
6 Laboratory for Cardiometabolic Research, University of Split School of Medicine, Šoltanska 2A, 21000 Split, Croatia
7 Faculty of Health Studies, University of Split, Ruđera Boškovića 35, 21000 Split, Croatia; dsupe@kbsplit.hr
8 Department of Laboratory Diagnostics, University Hospital of Split, Spinčićeva 1, 21000 Split, Croatia
* Correspondence: josko.bozic@mefst.hr

Abstract

Background/Objectives: Circulating dephosphorylated-uncarboxylated matrix Gla protein (dp-ucMGP) is influenced by vitamin K status, but its relationship with colorectal cancer (CRC) characteristics is poorly understood. We examined associations with tumour histopathology, location and host factors, as well as postoperative changes. Methods: This single-centre prospective cohort included 67 patients with newly diagnosed CRC scheduled for elective surgery. Plasma dp-ucMGP was measured by chemiluminescence immunoassay. Histopathological analyses focused on 58 patients without neoadjuvant therapy, of whom 31 had paired baseline and postoperative day-28 samples. Analyses used non-parametric tests and multivariable regression, with correction for multiple testing. Results: Median dp-ucMGP was highest in rectal cancer (630 pmol/L), compared with right- and left-sided colon cancer (481 and 455 pmol/L, respectively; overall q = 0.005). After adjustment for age, sex and estimated glomerular filtration rate (eGFR), the geometric mean was 49.4% higher in rectal than in right-sided colon cancer (95% CI, 22.6–81.9%). Among patients with available histopathology, the median was higher with perineural invasion (n = 8) than without it (n = 43; 753.5 versus 483 pmol/L; q = 0.048), but the association did not meet the corrected threshold after adjustment for location and eGFR (q = 0.144). Neither pathological T nor N category met the corrected threshold. No significant change was detected between baseline and day 28 (612 versus 593 pmol/L; p = 0.674). Conclusions: Plasma dp-ucMGP varied by tumour location in this exploratory cohort. The findings do not establish an independent association with invasive features or a role in staging or postoperative monitoring.

Keywords: colorectal cancer; matrix Gla protein; vitamin K; perineural invasion; tumour location; renal function; circulating biomarker

Academic Editor: Antonio Artigas

Received: 5 November 2026
Revised: 20 November 2026
Accepted: 21 November 2026
Published: 23 November 2026

Copyright: © 2026 by the authors. Licensee MDPI, Basel, Switzerland. This article is an open access article distributed under the terms and conditions of the Creative Commons Attribution (CC BY) license.

1. Introduction

Colorectal cancer (CRC) is a leading cause of cancer-related death worldwide [1]. Right-sided, left-sided and rectal tumours differ in molecular profile, treatment and prognosis [2,3]. Pathological T and N categories remain central to postoperative risk assessment, whereas carcinoembryonic antigen (CEA) and carbohydrate antigen 19-9 (CA19-9) have limited sensitivity and do not directly measure local tumour extent [4]. Circulating markers of tumour biology or relevant host responses therefore warrant investigation.

Matrix Gla protein (MGP) is a vitamin K-dependent inhibitor of ectopic mineralisation, as demonstrated by severe arterial and cartilage calcification in Mgp-deficient mice [5]. Its dephosphorylated-uncarboxylated form (dp-ucMGP) lacks both phosphorylation and γ-carboxylation and is inactive with respect to MGP's anti-calcific function [6,7]. Circulating dp-ucMGP is commonly interpreted as a marker of poor extrahepatic vitamin K status or insufficient MGP activation, and vitamin K2 supplementation reduces its concentration [8]. It does not directly measure vitamin K concentration or tumour MGP expression.

Circulating dp-ucMGP concentrations increase as renal function declines [9,10] and may also be influenced by age, vascular and metabolic disease, inflammation, nutritional status and body composition. These systemic determinants should be considered when interpreting associations with tumour characteristics, as such associations alone cannot establish tumour production or a causal role in progression.

CRC studies have reported both reduced MGP messenger RNA [11] and increased or dysregulated expression, with proposed roles in calcium-dependent NF-κB signalling, proliferation, oxaliplatin resistance and immune escape [12–15]. These tissue and experimental findings do not establish the origin of plasma dp-ucMGP. Human evidence on circulating MGP species in CRC remains sparse: one study reported increased uncarboxylated MGP but limited discrimination of metastatic disease [16].

This prospective cohort study investigated plasma dp-ucMGP as a potential marker of tumour characteristics and postoperative change in patients with newly diagnosed CRC scheduled for elective surgery. In patients without neoadjuvant therapy, we examined its associations with histopathological features. We also explored relationships with tumour location, body composition and laboratory parameters across the full cohort. Changes 28 days after surgery were assessed using paired samples from patients who had not received neoadjuvant therapy.

2. Materials and Methods

2.1. Study Design, Setting, and Ethical Approval

This single-centre prospective observational cohort study was conducted at the Department of Abdominal Surgery, Clinic of Surgery, University Hospital of Split, in collaboration with the University of Split School of Medicine. Recruitment and follow-up took place from April 2023 to November 2025. The main objective was to examine the association between baseline plasma dp-ucMGP and tumour histopathological features. Additional exploratory analyses examined associations with tumour location, body composition and laboratory parameters, as well as postoperative changes in dp-ucMGP.

The study protocol and amendments were approved by the Ethics Committee of KBC Split (Class: 500-03/23-01/33; No. 2181-147/01/06/L.Z.-23-02, 28 February 2023; No. 2181-147/01-06/LJ.Z.-24-05, 24 October 2024; and No. 2181-147/01-06/LJ.Z.-26-05, 26 June 2026). All participants provided written informed consent before study-specific procedures. Clinical data were entered into a de-identified study database and analysed in accordance with the Declaration of Helsinki.

2.2. Participants and Assessment Schedule

Eligible participants were adults aged 18–80 years with newly diagnosed, histologically confirmed colorectal cancer who were scheduled for elective surgical treatment. Patients were recruited according to availability and willingness to provide written informed consent. Exclusion criteria included previously reported chronic kidney disease, the need for emergency surgery, use of vitamin K antagonists, malabsorption disorders, vitamin K supplementation, and liver disease. Patients with metastatic or recurrent disease and those undergoing palliative procedures were also excluded. Before enrolment, all participants had undergone diagnostic colonoscopy with biopsy or endoscopic resection; these diagnostic procedures were distinguished from neoadjuvant oncological treatment. The analytical cohort comprised all 67 enrolled participants, each with an observed baseline dp-ucMGP measurement.

Baseline measurements and routine laboratory covariates were obtained after histological confirmation, 2–3 weeks before surgery in the 58 patients without neoadjuvant therapy and before chemoradiotherapy in the nine who received it. Prior diagnostic biopsy or endoscopic resection did not constitute neoadjuvant therapy. Postoperative assessment was on day 28, before adjuvant treatment.

Principal histopathological analyses, including multivariable models, excluded nine neoadjuvant chemoradiotherapy recipients, leaving 58 eligible patients without neoadjuvant therapy. Tumour-location, physiology and body-composition analyses used the full cohort, with variable-specific availability.

Longitudinal analyses excluded the nine neoadjuvantly treated patients: 31 of the remaining 58 had paired baseline/day-28 measurements, while 27 did not provide a follow-up sample and had baseline values only.

2.3. Clinical, Surgical, and Postoperative Variables

Age and sex were recorded. Tumour location was recorded by bowel segment and grouped as right colon (caecum, ascending colon and proximal two thirds of the transverse colon), left colon (distal third of the transverse colon, descending colon and sigmoid colon), or rectum.

Additionally, surgical procedure, approach, stoma formation, postoperative days of urinary-catheter removal and first stool, and hospital stay were recorded.

Major and minor complications were defined using the study event categories and were recorded during the first 28 postoperative days. Major categories were ileus requiring nasogastric-tube placement and assessment by the surgeon, anastomotic dehiscence, wound dehiscence, a combined intra-abdominal abscess or haemoperitoneum category, and other. Minor categories were wound infection, wound haematoma, vomiting and other. Binary complication indicators denoted at least one event in the corresponding category; major and minor indicators were not mutually exclusive.

Reoperation and readmission were recorded within 30 days after discharge; mortality denoted death during the index hospitalisation.

2.4. Body Composition and Derived Indices

Body composition was assessed using a Tanita MC-780 bioelectrical impedance analyser (Tanita Corporation, Tokyo, Japan) and GMON software, version 3.4.8 (Medizin & Service GmbH, Chemnitz, Germany) [17]. Recorded measures included body mass and composition, water compartments, impedance and phase angle. Device-estimated whole-body muscle mass was analysed in kilograms and includes skeletal and nonskeletal muscle tissues and their water content according to the manufacturer's definition.

Body height was measured using the integrated stadiometer of a calibrated medical scale (Seca, Birmingham, UK). Body mass index (BMI) was calculated as body weight in

kilograms divided by measured height in metres squared. Fat-free mass, fat mass, and whole-body muscle mass were divided by reconstructed height squared to calculate the fat-free mass index (FFMI), fat mass index (FMI), and whole-body muscle mass index, respectively. All indices were expressed in kg/m^2.

Hydration indices were extracellular water/total body water (ECW/TBW), extracellular water/intracellular water (ECW/ICW), and total body water/fat-free mass. ECW/TBW and ECW/ICW are monotonically related when total body water equals the sum of its extracellular and intracellular compartments; they were not regarded as independent confirmations.

2.5. Histopathological and Routine Laboratory Assessment

Histopathological examination was performed at the Department of Pathology, University Hospital of Split. Biopsy and resection specimens underwent fixation, automated dehydration, paraffin embedding and microtome sectioning. Tissue sections were stained with haematoxylin and eosin using an automated staining system and examined by light microscopy. Histopathological variables were extracted from the diagnostic biopsy or endoscopic resection reports and verified against the definitive surgical pathology reports. Variables included T/N stage, positive and examined lymph-node counts, grade, lymphovascular invasion and perineural invasion. Staging followed the eighth edition of the AJCC TNM classification, using reported stage or, when unavailable, verified descriptive findings [18].

Histological grade was recorded as low or high based on the original pathology report. The reported categories were used directly in the statistical analyses, without further reclassification. Count-derived lymph-node positivity was defined as at least one positive node and was analysed separately from pathological N stage.

Baseline serum creatinine concentrations were measured using the Creatinine plus ver. 2 enzymatic colorimetric assay on a cobas c 703 analyser (Roche Diagnostics GmbH, Mannheim, Germany) and reported in μmol/L. Calibration was traceable to isotope-dilution mass spectrometry. Estimated glomerular filtration rate (eGFR) was calculated with the 2009 creatinine-based Chronic Kidney Disease Epidemiology Collaboration (CKD-EPI) equation and expressed in mL/min/1.73 m^2. The C-reactive protein-to-albumin ratio (CAR) was calculated as CRP (mg/L) divided by albumin (g/dL), converting albumin from g/L by division by 10.

2.6. Measurement of dp-ucMGP

Peripheral venous blood was collected at baseline and postoperative day 28; baseline preceded neoadjuvant chemoradiotherapy where applicable. A portion of each sample was used for routine clinical laboratory testing. Plasma was stored at −80 °C until analysis. Plasma dephosphorylated-uncarboxylated matrix Gla protein (dp-ucMGP) was measured by chemiluminescence immunoassay (CLIA) using the IDS-iSYS InaKtif MGP assay (IDS Immunodiagnostic Systems GmbH, Frankfurt am Main, Germany), according to the manufacturer's instructions. Concentrations were reported in pmol/L.

The assay limits of blank (LoB), detection (LoD) and quantitation (LoQ) were 100, 200 and 300 pmol/L, respectively. Linearity over 300–12,000 pmol/L was evaluated by the manufacturer in accordance with CLSI EP-6A (Immunodiagnostic Systems Limited, Boldon, UK). The reported precision assessment included three kit controls and four plasma samples, each analysed in duplicate twice daily for 20 days. Coefficients of variation were 8.2%, 3.4% and 3.3% for kit controls 1–3, respectively, and 7.9%, 4.8%, 3.5% and 3.0% for plasma samples 1–4, respectively.

2.7. Statistical Analysis

Analyses were performed in R version 4.6.0. Continuous variables are reported as mean ± SD or median (IQR), and categorical variables as n (%). Distributions were assessed graphically and using Shapiro–Wilk tests. Available observations were analysed without imputation. Independent groups were compared using Mann–Whitney or Kruskal–Wallis tests, with an exact permutation Mann–Whitney test for histological grade. Correlations were assessed using Spearman's coefficient, with supplementary Pearson analyses. Rank-based 95% confidence intervals were estimated using 5000 percentile-bootstrap resamples.

Multivariable associations were examined using complete-case linear models of log-transformed dp-ucMGP. Back-transformed coefficients were expressed as percentage differences in conditional geometric means. Model diagnostics assessed residual distributions, heteroscedasticity, collinearity and influential observations. Sensitivity analyses included additional covariate adjustment, HC3 robust inference and influence checks.

Baseline and postoperative day-28 concentrations in 31 patients were compared using the paired Wilcoxon signed-rank test. Baseline characteristics were compared by follow-up availability using Mann–Whitney, chi-square or Fisher's exact tests. Benjamini–Hochberg correction was applied separately within analytical domains and model families, with Holm adjustment for pairwise comparisons. For multilevel pathological categories, exploratory pairwise comparisons were considered only after a nominally significant overall test. All tests were two-sided; BH $q < 0.05$ or Holm-adjusted $p < 0.05$ defined statistical significance. Uncorrected $p < 0.05$ was considered nominal when the corresponding multiplicity-adjusted threshold was not met.

3. Results

3.1. Study Population and Baseline Characteristics

The cohort comprised 67 patients with a median age of 64 (57–69) years; 42 (62.7%) were male. Tumours were located in the right colon in 17 (25.4%), left colon in 27 (40.3%) and rectum in 23 (34.3%) patients. Nine patients, all with rectal cancer, received neoadjuvant chemoradiotherapy after baseline sampling. During the first 28 postoperative days, major and minor complications occurred in 6 (9.0%) and 26 (38.8%) patients, respectively, with 4 (6.0%) experiencing both.

Mean BMI and fat mass index were 26.18 ± 4.79 and 6.82 ± 3.21 kg/m^2, respectively. Median fat-free mass index was 19.55 (17.10–21.36) kg/m^2, and median phase angle was 5.47 (5.05–5.98)°. Clinical, surgical and body-composition characteristics are summarised overall and by sex in Table 1.

Table 1. Clinical, surgical and selected body-composition characteristics.

Characteristic	Overall (N = 67)	Male (n = 42)	Female (n = 25)
Age, years	64.00 (57.00–69.00)	63.00 (56.50–67.75)	68.00 (60.00–70.00)
Tumor location			
Right colon	17 (25.4%)	11 (26.2%)	6 (24.0%)
Left colon	27 (40.3%)	17 (40.5%)	10 (40.0%)
Rectum	23 (34.3%)	14 (33.3%)	9 (36.0%)
Body mass index, kg/m^2	26.18 ± 4.79	26.94 ± 4.83	24.94 ± 4.56
Fat-free mass index, kg/m^2	19.55 (17.10–21.36)	21.20 (19.51–22.10)	16.41 (15.52–17.30)
Fat mass index, kg/m^2	6.82 ± 3.21	6.09 ± 3.22	8.05 ± 2.86
Phase angle, °	5.47 (5.05–5.98)	5.75 (5.33–6.17)	5.08 (4.60–5.52)
Surgical procedure:			

Right/extended right hemicolectomy	17 (25.4%)	11 (26.2%)	6 (24.0%)
Left colectomy	7 (10.4%)	4 (9.5%)	3 (12.0%)
Hartmann procedure	1 (1.5%)	0 (0.0%)	1 (4.0%)
Low anterior resection/Dixon	34 (50.7%)	22 (52.4%)	12 (48.0%)
Abdominoperineal resection	7 (10.4%)	4 (9.5%)	3 (12.0%)
Transanal minimally invasive surgery (TAMIS)	1 (1.5%)	1 (2.4%)	0 (0.0%)
Stoma formation	16 (23.9%)	10 (23.8%)	6 (24.0%)
Operative approach:			
Open/classic	36 (53.7%)	23 (54.8%)	13 (52.0%)
Laparoscopic	31 (46.3%)	19 (45.2%)	12 (48.0%)
Urinary catheter removal, postoperative day	3.00 (2.00–4.00)	3.00 (2.00–4.00)	3.00 (2.00–4.00)
First stool, postoperative day	4.00 (2.00–5.00)	4.00 (3.00–5.00)	4.00 (2.00–5.00)
Postoperative hospital stay, days	7.00 (5.00–7.00)	7.00 (5.00–8.00)	7.00 (5.00–7.00)
Any major complication	6 (9.0%)	3 (7.1%)	3 (12.0%)
Any minor complication	26 (38.8%)	14 (33.3%)	12 (48.0%)
Reoperation	5 (7.5%)	3 (7.1%)	2 (8.0%)
Readmission within 30 days	7 (10.4%)	3 (7.1%)	4 (16.0%)

Values are mean ± SD, median (IQR), or n (%). Available n (overall/male/female): BMI, 61/38/23; FFMI and FMI, 59/37/22 each; phase angle, 62/38/24; urinary catheter removal, 62/41/21; first stool, 57/36/21; and hospital stay, 66/41/25. All other characteristics had complete data (67/42/25). Percentages use the corresponding column denominator.

Mean hemoglobin concentration was 132 ± 18.6 g/L, and median eGFR was 89 (80.9–96.4) mL/min/1.73 m^2. Median CEA and CA19-9 concentrations were 3.25 (2.02–5.62) µg/L and 9.32 (5.96–14.95) kIU/L, respectively. The median baseline plasma dp-ucMGP concentration was 508 (383.5–643.5) pmol/L. Baseline laboratory and biomarker concentrations are summarised overall and by sex in Table 2.

Table 2. Baseline laboratory and biomarker concentrations.

Characteristic	Overall (N = 67)	Male (n = 42)	Female (n = 25)
WBC, 10^9/L	6.65 (5.2–8.18)	6.7 (5.2–8)	6.6 (5.2–8.6)
Hemoglobin, g/L	132 ± 18.6	134.5 ± 21.1	127.8 ± 12.9
Platelet count, 10^9/L	248 (202–295)	237 (197.25–273.25)	269 (213–317)
C-reactive protein, mg/L	2.55 (0.68–14.55)	8.2 (2.5–25.1)	0.8 (0.6–4.65)
Creatinine, µmol/L	77.5 (62.75–84)	81 (75–88)	62 (57.5–75)
Estimated glomerular filtration rate, mL/min/1.73 m^2	89 (80.9–96.4)	90.6 (83.48–96.7)	88 (72.7–96.4)
Total protein, g/L	67.5 (63–71)	68 (63–71)	66 (64–72)
Albumin, g/L	42.3 (40.1–45)	42.75 (40.18–45.82)	41.6 (39.9–44)
Carcinoembryonic antigen (CEA), µg/L	3.25 (2.02–5.62)	2.65 (1.83–4.47)	4.02 (3.18–6.79)
Carbohydrate antigen 19-9 (CA19-9), kIU/L	9.32 (5.96–14.95)	8.26 (4.75–13.15)	9.42 (7.33–20.6)
Baseline plasma dp-ucMGP, pmol/L	508 (383.5–643.5)	538.5 (413.75–646.75)	502 (357–619)

Values are mean ± SD for hemoglobin and median (IQR) for all other variables. Available n (overall/male/female): WBC and total protein, 58/37/21 each; hemoglobin, 61/38/23; platelets, 63/40/23; C-reactive protein, 24/12/12; creatinine, 60/37/23; eGFR, 59/36/23; albumin, 57/36/21; CEA, 66/42/24; and CA19-9 and dp-ucMGP, 67/42/25 each.

Among the 58 patients without neoadjuvant therapy, pT3 was the most frequent T category (35/58; 60.3%), and 18/58 (31.0%) had node-positive disease. Most tumours were low grade (48/50; 96.0%), while lymphovascular and perineural invasion were present in 12/51 (23.5%) and 8/51 (15.7%) patients, respectively. Detailed histopathological characteristics are reported in Table S1.

3.2. Associations with Histopathological Characteristics

Figure 1a shows overlapping dp-ucMGP concentrations across pathological T categories (overall $p = 0.214$, q = 0.241). In Figure 1b, the median was highest in N2 disease, but the overall N-category comparison did not meet the corrected threshold ($p = 0.049$, q = 0.132). Figure 1c shows higher concentrations with perineural invasion (n = 8) than without it (n = 43): 753.5 (662.0–841.75) versus 483.0 (340.5–612.0) pmol/L. The rank-biserial correlation was 0.628 (95% CI, 0.122 to 0.953; $p = 0.005$, q = 0.048). In Figure 1d, concentrations were higher in the two patients with high-grade tumours than in the low-grade group, but the comparison did not meet the corrected threshold (exact permutation $p = 0.019$, q = 0.084). Count-derived nodal positivity and the numbers of positive or examined nodes likewise did not meet the histopathology FDR threshold (Table 3).

Table 3. Associations between baseline dp-ucMGP and histopathology in patients without neoadjuvant therapy.

Characteristic	n	dp-ucMGP, pmol/L; Median (IQR)	Effect (95% CI Where Estimated)	*p*	BH q
Pathological T stage (pT only)	58	T1 (n = 8): 499.50 (433.00–595.75); T2 (n = 9): 650.00 (589.00–710.00); T3 (n = 35): 483.00 (325.50–614.50); T4 (n = 6): 535.00 (382.25–699.75)	$\varepsilon^2 = 0.027$	0.214	0.241
Pathological N stage (pN only)	58	N0 (n = 40): 494.50 (440.00–608.25); N1 (n = 12): 511.00 (315.50–621.25); N2 (n = 6): 753.50 (691.75–814.50)	$\varepsilon^2 = 0.073$	0.049	0.132
Count-derived lymph-node positivity	58	Node-negative (n = 40): 494.50 (440.00–608.25); Node-positive (n = 18): 614.50 (326.75–762.25)	$r_{r\beta} = 0.189$ (−0.195 to 0.558)	0.257	0.257
Number of positive lymph nodes, all patients	58	Available-case continuous association	$\varrho = 0.201$ (−0.133 to 0.486)	0.130	0.234
Number of positive lymph nodes among node-positive patients	18	Available-case continuous association	$\varrho = 0.454$ (−0.024 to 0.778)	0.058	0.132
Number of examined lymph nodes	57	Available-case continuous association	$\varrho = -0.18$ (−0.43 to 0.09)	0.181	0.241
Histological grade	50	Low grade (n = 48): 494.50 (345.25–631.00); High grade (n = 2): 910.50 (840.75–980.25)	$r_{r\beta} = 0.896$ (0.667 to 1)	0.019	0.084
Lymphovascular invasion	51	No (n = 39): 491.00 (387.50–613.50); Yes (n = 12): 647.00 (386.50–785.50)	$r_{r\beta} = 0.252$ (−0.209 to 0.675)	0.194	0.241
Perineural invasion	51	No (n = 43): 483.00 (340.50–612.00); Yes (n = 8): 753.50 (662.00–841.75)	$r_{r\beta} = 0.628$ (0.122 to 0.953)	0.005	0.048

Concentrations are median (IQR), pmol/L; n is analysis-specific within 58 eligible patients without neoadjuvant therapy. BH q covers all nine listed tests. Positive binary effects denote second-listed minus first-listed groups; ε^2 is truncated at zero. Grade is descriptive because only two tumours were high grade. Pooled results are in Table S2.

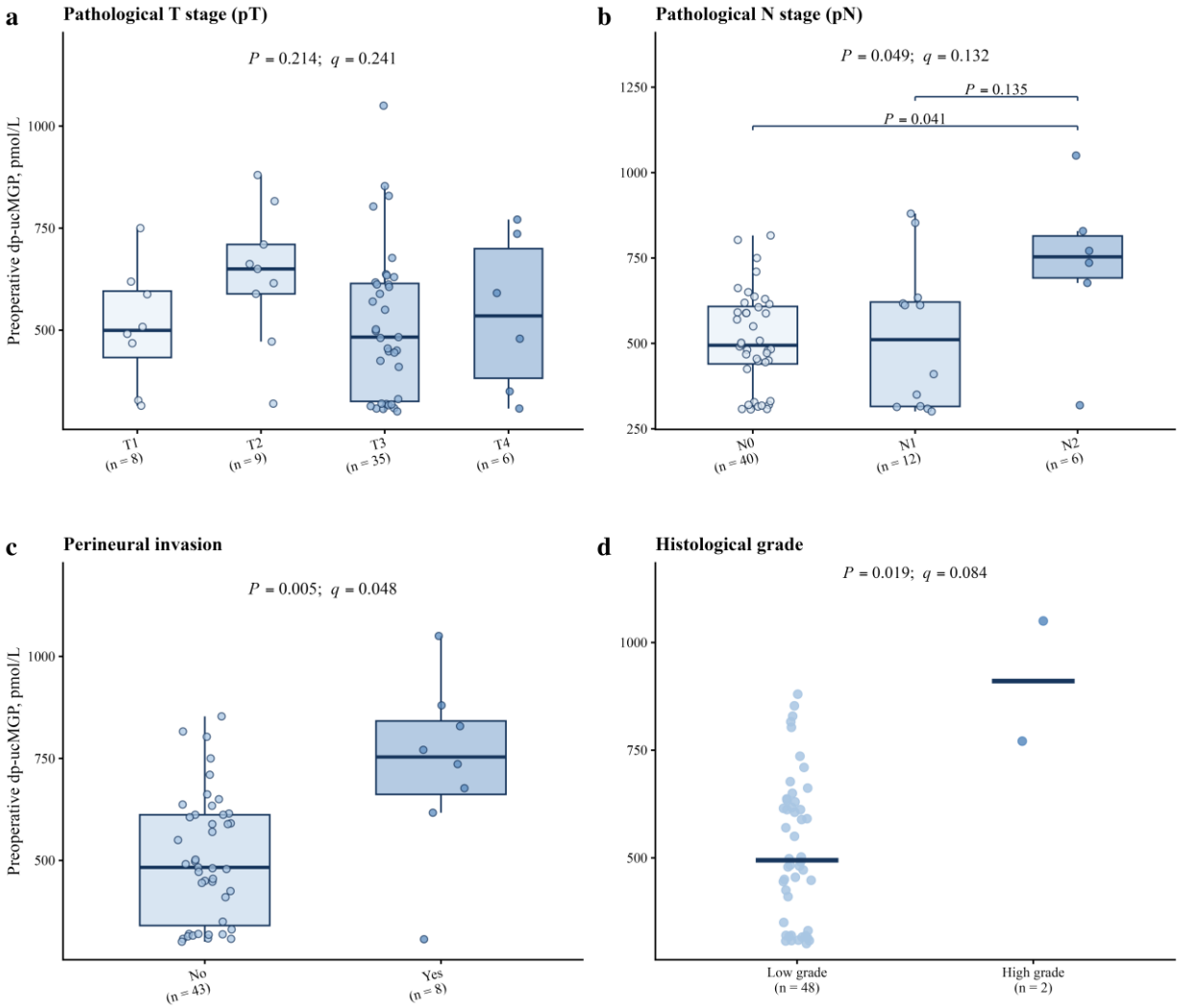


Figure 1. Baseline plasma dp-ucMGP concentrations according to histopathological characteristics in patients without neoadjuvant therapy: (**a**) pathological T category, (**b**) pathological N category, (**c**) perineural invasion and (**d**) histological grade. Points represent individual observations; group-specific sample sizes are shown. Boxes indicate medians and interquartile ranges, with whiskers extending to the most extreme observations within 1.5 interquartile ranges. Horizontal lines in panel (**d**) indicate medians. *p*-values were obtained using Kruskal–Wallis tests for T/N categories, the Mann–Whitney test for perineural invasion and an exact permutation Mann–Whitney test for grade. BH q-values refer to the nine-test histopathology family. Brackets in panel (**b**) indicate exploratory Holm-adjusted pairwise comparisons and do not supersede the non-significant overall FDR-adjusted result. The y-axis title on the left applies to both panels in each row. No pairwise *p*-values are shown in panel (**a**) because the overall T-category comparison was not nominally significant (p = 0.214).

3.3. dp-ucMGP and Tumour Location

Full-cohort median dp-ucMGP was 630.00 pmol/L in rectal, 481.00 in right-colon and 455.00 in left-colon tumours (ε^2 = 0.167; p = 0.002, q = 0.005; Figure 2; Table S3). Holm-adjusted comparisons showed higher concentrations in rectal than right-colon (p = 0.005) or left-colon tumours (p = 0.006); right- and left-colon tumours did not differ significantly (p = 0.857).

The overall location association remained significant after adjustment for age, sex and eGFR (n = 59; p < 0.001). Rectal location was associated with a 49.4% higher conditional geometric mean dp-ucMGP than right-colon location (95% CI 22.6% to 81.9%; p < 0.001).

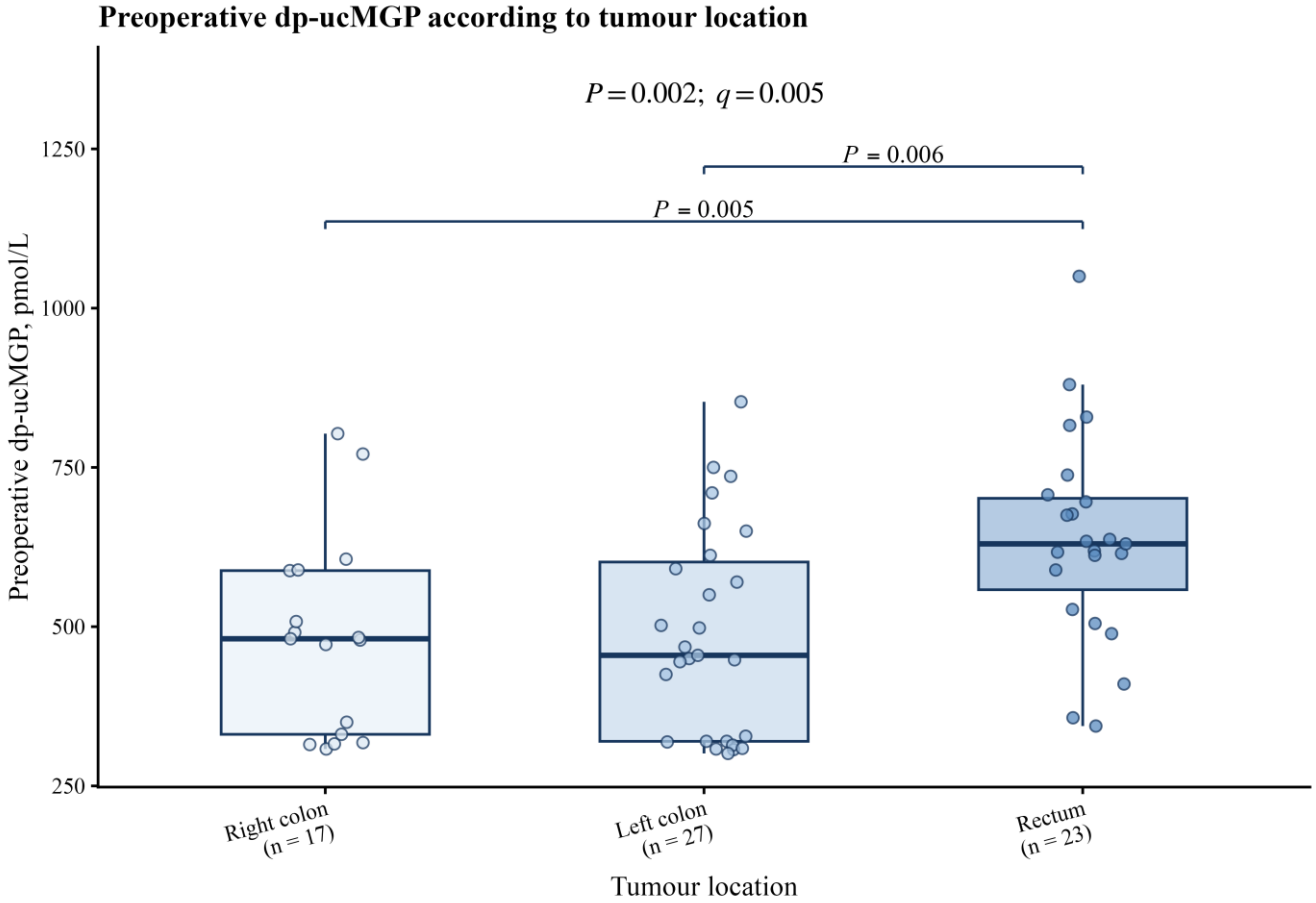


Figure 2. Baseline dp-ucMGP by tumour location. Points show all observations and labelled sample sizes; boxes show median and IQR, with 1.5-IQR whiskers. Overall Kruskal–Wallis $p = 0.002$ and three-marker BH q = 0.005; pairwise Mann–Whitney annotations are Holm adjusted.

3.4. Body-Composition and Laboratory Associations

No body-composition or nutritional correlation met the broad 24-test FDR threshold. Fat mass showed a nominal association ($\varrho = 0.256$; $p = 0.048$, q = 0.391). Complete estimates, confidence intervals and variable-specific sample sizes are in Table S4.

dp-ucMGP correlated positively with hemoglobin ($\varrho = 0.314$; 95% CI 0.072 to 0.526; $p = 0.014$) and inversely with eGFR ($\varrho = -0.299$; 95% CI −0.521 to −0.049; $p = 0.021$). Neither met the broad 14-test laboratory/clinical FDR threshold (q = 0.150 for both).

There were no nominal correlations with CEA or CA19-9. The complete laboratory/clinical domain, including creatinine, is reported in Table S5.

3.5. Multivariable Analyses of dp-ucMGP

In adjusted log-dp-ucMGP models, each 10 mL/min/1.73 m^2 higher eGFR corresponded to a 5.9% lower conditional geometric mean ($p = 0.031$, q = 0.031), and each 10 g/L higher hemoglobin to a 6.6% higher concentration ($p = 0.010$, q = 0.021). The hemoglobin estimate remained 6.6% after location adjustment. Table 4 reports the adjustment sets, effect estimates and confidence intervals.

The model for perineural invasion (PNI), adjusted for tumour location and eGFR, included 44 patients without neoadjuvant therapy (seven positive, 37 negative). Its estimate was 30.4% (95% CI 2.9% to 65.3%; $p = 0.029$, q = 0.144), failing the five-target pathology FDR threshold. Age/sex expansion also failed this threshold (q = 0.259). No pathology or body-composition target met its model-family threshold (Tables 4 and S6–S8). HC3 inference for the original adjusted PNI model gave an interval including no difference

(−3.3% to 76%; $p = 0.081$, q = 0.286). Uniform sensitivities are reported in Tables S6–S8, and node-count influence checks in Table S9.

Table 4. Adjusted models of preoperative dp-ucMGP concentrations.

Predictor	Population	Adjustment Set	Adjusted R^2	Relative Difference (95% CI)	*p*	BH q
Estimated glomerular filtration rate, per 10 mL/min/1.73 m²	Full cohort	Age, sex, tumour location	0.295	−5.9 (−10.9 to −0.6)%	0.031	0.031
Hemoglobin, per 10 g/L	Full cohort	Age, sex, eGFR	0.122	6.6 (1.6 to 11.9)%	0.010	0.021
Hemoglobin, per 10 g/L (location sensitivity)	Full cohort	Age, sex, eGFR, tumour location	0.389	6.6 (2.2 to 11.2)%	0.003	—
Perineural invasion present	Patients without neoadjuvant therapy	Tumour location, eGFR	0.451	30.4 (2.9 to 65.3)%	0.029	0.144
Lymphovascular invasion present	Patients without neoadjuvant therapy	Tumour location, eGFR	0.401	13.8 (−7.8 to 40.6)%	0.223	0.297
Pathological node-positive stage (pN)	Patients without neoadjuvant therapy	Tumour location, eGFR	0.382	4.9 (−12.7 to 25.9)%	0.603	0.603
Advanced pathological T stage (pT3–pT4)	Patients without neoadjuvant therapy	Tumour location, eGFR	0.414	−12.5 (−25.6 to 2.9)%	0.104	0.261
Fat-free mass index, per kg/m²	Full cohort	FMI, age, sex	0.133	−6.5 (−12.4 to −0.3)%	0.042	0.083
Fat mass index, per kg/m²	Full cohort	FFMI, age, sex	0.133	5.2 (1.1 to 9.5)%	0.014	0.058
Phase angle, per degree	Full cohort	Body mass index, age, sex	0.047	−4.1 (−14.1 to 7.1)%	0.450	0.450
Body mass index, per kg/m²	Full cohort	Phase angle, age, sex	0.047	1.1 (−0.8 to 3)%	0.248	0.330

Effects are relative differences in conditional geometric means, 100 × [exp(β) − 1], with two-sided t inference. Separate BH families comprise two physiology targets, five pathology targets in patients without neoadjuvant therapy, and four body-composition targets (Table S10). The location-augmented hemoglobin sensitivity has no separate q. Combined invasion and uniform conventional/HC3 sensitivities are in Tables S6–S8. Both adjusted PNI models include seven positive and 37 negative patients.

3.6. Preoperative-to-Postoperative Change in dp-ucMGP

Among the 31 patients with paired measurements, median plasma dp-ucMGP concentrations were 612 (494.5–723) versus 593 (473.5–714.5) pmol/L at baseline and postoperative day 28, respectively, with no statistically significant paired change ($p = 0.674$; Figure 3).

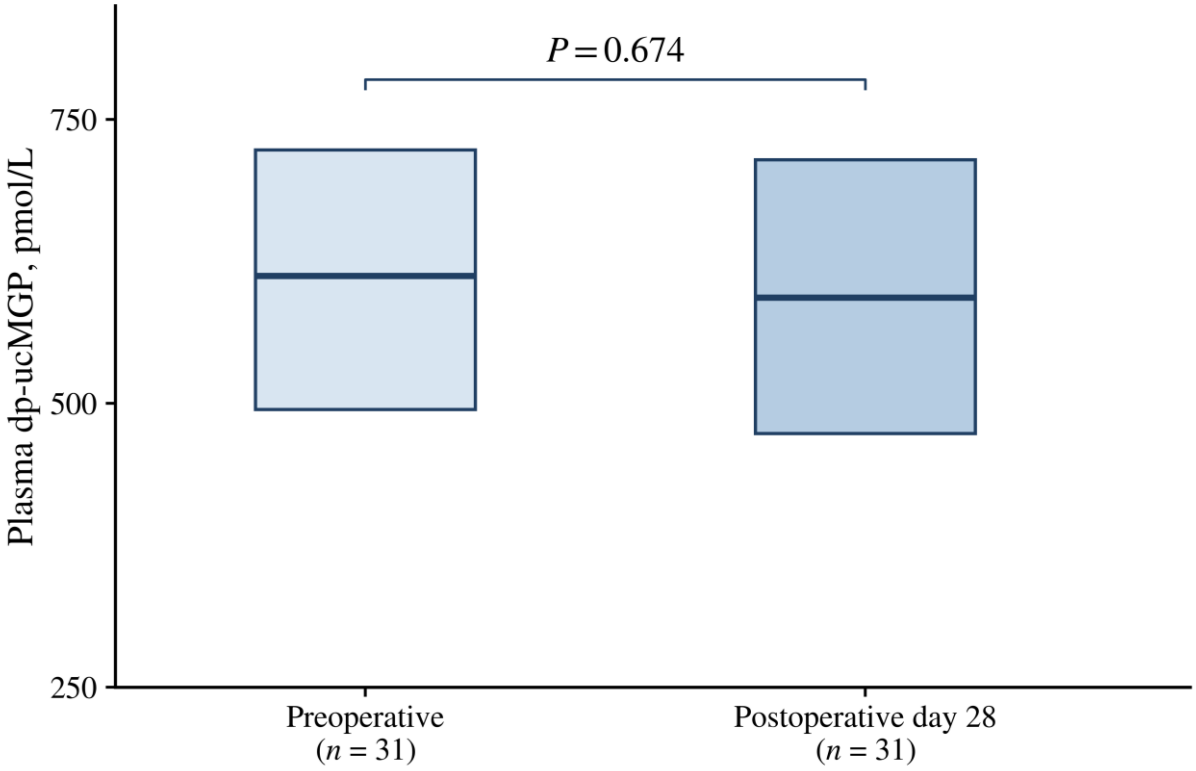


Figure 3. Plasma dp-ucMGP before surgery and on postoperative day 28 in 31 patients without neoadjuvant therapy. Boxes indicate IQRs, with horizontal lines representing medians.

4. Discussion

Among patients scheduled for elective colorectal cancer surgery, plasma dp-ucMGP was highest in those with rectal cancer. The overall association with tumour location persisted after adjustment for age, sex and eGFR. Histopathology provided a less consistent picture: perineural invasion was associated with higher concentrations in the unadjusted comparison, but no pathology association met the corrected threshold in the adjusted models.

The location association persisted after adjustment for age, sex and eGFR, supporting its relevance beyond the unadjusted comparison and providing a rationale for further studies stratified by tumour location. All nine neoadjuvant recipients had rectal cancer and were sampled before chemoradiotherapy; direct exposure to that treatment therefore cannot explain their baseline values. However, treatment indication, disease extent and patient selection may still confound the comparison. No location analysis restricted to the 58 patients without neoadjuvant therapy is reported, so persistence of the association in that group is unknown. Anatomical differences in CRC biology [2,3] raise the possibility that tissue MGP expression or its release into the circulation differs by site. A higher plasma concentration could also reflect a larger fraction of MGP remaining uncarboxylated at a similar level of tissue expression. Neither mechanism can be distinguished here: no paired tumour and adjacent-mucosa specimens were assayed for MGP. For future comparisons, the immediate implication is to account for tumour site and the indication for neoadjuvant therapy when interpreting a plasma value.

The distinction between tissue MGP and circulating dp-ucMGP is fundamental. CRC studies have reported both reduced MGP expression [11] and increased or pro-tumoural signalling [12–15], potentially reflecting differences in platforms, compartments and measured species. Plasma dp-ucMGP is one inactive post-translational form influenced by vitamin K-dependent activation and systemic handling [6–10]. Comparisons across

studies should account for the MGP form measured and the assay used [16]. Paired assessment of plasma dp-ucMGP and tumour MGP expression would help clarify how circulating concentrations relate to tissue findings.

Perineural invasion was the only histopathological feature that met the multiplicity threshold in the univariable analysis. Only eight patients had documented invasion, and seven contributed to the adjusted analysis. Although the adjusted estimate remained positive, it did not survive correction for multiple testing, and the robust confidence interval included no difference. The result identifies a question for a larger series rather than evidence that plasma dp-ucMGP independently marks invasive disease. The positive-node correlation was sensitive to one observation, and the two high-grade tumours were too few for a reliable grade comparison.

The inverse eGFR association agrees with findings in healthy, diabetic, chronic-kidney-disease and transplant populations [9,10,19]. Each 10 mL/min/1.73 m^2 higher eGFR was associated with a 5.9% lower conditional geometric mean dp-ucMGP. Haemoglobin requires greater caution: positive associations have been reported in a selected healthy reference population [9], but inverse associations across chronic kidney disease stages [19]. Although our adjusted estimate persisted after location adjustment, the univariable result failed the broad laboratory/clinical correction. These findings highlight the value of considering renal function and haematological variables when interpreting circulating dp-ucMGP and designing subsequent biomarker studies in CRC.

Other non-cancer evidence reinforces the importance of host context. Higher dp-ucMGP has been associated with kidney dysfunction and arterial stiffness and with subsequent renal deterioration [20,21]. Brnic et al. reported elevated dp-ucMGP and inflammatory-marker associations in inflammatory bowel disease using the same IDS-iSYS InaKtif MGP platform [22], whereas a later Crohn's disease cohort found no associations with endoscopic activity, faecal calprotectin or C-reactive protein [23]. The broader interplay of dysbiosis, inflammation, endothelial dysfunction and cardiovascular risk reviewed in inflammatory bowel disease [24] is relevant context, but neither these observations nor our data establish an inflammatory mechanism for dp-ucMGP in CRC.

Host phenotype provides further context: general-population studies associate dp-ucMGP with obesity, blood pressure, vascular measures and metabolic or renal disease [25,26], while magnetic-resonance imaging in hypertension links higher concentrations to lower axial skeletal-muscle mass [27]. In our cohort, no body-composition association met the corresponding threshold after correction for multiple testing.

Among the 31 patients who provided both samples, we detected no paired change by postoperative day 28. A single follow-up measurement cannot exclude an earlier or later change, and the result does not establish equivalence or demonstrate that dp-ucMGP can monitor residual disease. Vitamin K supplementation has been shown to reduce circulating dp-ucMGP [8]. Supplement use was an exclusion criterion, but this did not quantify habitual dietary intake or establish cumulative exposure to supplements before enrolment. Vitamin K intake and status were not measured directly. Patients with similar tumour features could therefore have different dp-ucMGP concentrations because of differences in vitamin K availability or renal function. Adjustment for eGFR addresses only the latter, and does not separate tumour production from these systemic influences.

The clinical question is whether dp-ucMGP adds information beyond tumour site, pathological stage and established markers. We did not compare the performance of clinical models with and without dp-ucMGP, and the study was not designed to assess recurrence or survival. The absence of a correlation with CEA or CA19-9 does not in itself demonstrate added value. A larger cohort with prospectively recorded treatment indications, dietary vitamin K intake and serial blood samples could test whether dp-ucMGP adds to established predictors of recurrence.

Prospective baseline sampling before oncological treatment and separate analyses of patients without neoadjuvant therapy helped distinguish pretreatment concentrations from changes following treatment. Reporting the adjusted estimates alongside analyses using robust standard errors illustrates the uncertainty around the perineural invasion finding.

Limitations include the small, single-centre availability sample, sparse subgroups and analysis-defined models. Eligibility exclusions restrict generalisability, and dietary vitamin K intake, direct vitamin K status and several host determinants were unavailable. Variable-specific availability reduced model samples, and follow-up selection limits longitudinal inference.

5. Conclusions

Baseline plasma dp-ucMGP was highest in rectal cancer in this cohort. The overall association with tumour location persisted after adjustment for age, sex and renal function. The association with perineural invasion was confined to the univariable analysis after correction for multiple testing. These findings make tumour site and renal function relevant to the design of future studies; they do not establish that dp-ucMGP improves CRC staging, risk stratification or postoperative monitoring.

Supplementary Materials: The following supporting information can be downloaded at: https://www.mdpi.com/article/10.3390/medsci14080808/s1, The accompanying Supplementary Materials file contains the following tables: Table S1: Histopathological characteristics of the primary and pooled populations; Table S2: Pooled histopathology associations with baseline dp-ucMGP; Table S3: Tumour-location comparisons across three biomarkers; Table S4: Complete correlations with body composition and nutritional indices; Table S5: Complete correlations with laboratory and clinical variables; Table S6: Pathology models in patients without neoadjuvant therapy with conventional and HC3 inference; Table S7: Age- and sex-expanded pathology models with conventional and HC3 inference; Table S8: eGFR-expanded body-composition models with conventional and HC3 inference; Table S9: Influence of one observation on the positive-node correlation in patients without neoadjuvant therapy; Table S10: Multiplicity families for the tabulated analyses.

Author Contributions: Conceptualization, I.O. and J.B.; methodology, I.O., I.M., D.Š.D. and J.B.; formal analysis, R.Š. and M.K.; investigation, I.O., I.M., P.M.Ž. and D.Š.D.; data curation, I.O., P.M.Ž. and R.Š.; writing—original draft preparation, I.O.; writing—review and editing, I.O., I.M., R.Š., P.M.Ž., D.Š.D., M.K. and J.B.; visualization, I.O. and R.Š.; supervision, J.B.; project administration, I.O. and J.B. All authors have read and agreed to the published version of the manuscript.

Funding: This research was funded by the European Union (NextGenerationEU) under the Croatian Recovery and Resilience Plan 2021–2026 (NRRP), through the University of Split institutional project "Personalized Medicine in IBD: Integration of Clinical, Laboratory, and AI Models for Outcome Prediction" (AI-IBD; IP-UNIST-32), approved by the Ministry of Science, Education and Youth of the Republic of Croatia.

Institutional Review Board Statement: The study was conducted in accordance with the Declaration of Helsinki. The study protocol was approved by the Ethics Committee of the University Hospital of Split (KBC Split; Class: 500-03/23-01/33; No. 2181-147/01/06/L.Z.-23-02, 28 February 2023; No. 2181-147/01-06/LJ.Z.-24-05, 24 October 2024; and No. 2181-147/01-06/LJ.Z.-26-05, 26 June 2026).

Informed Consent Statement: Informed consent was obtained from all subjects involved in the study.

Data Availability Statement: The data presented in this study are available upon request to the corresponding author. The data are not publicly available because some of the data sets will be used for further research.

Conflicts of Interest: The authors declare no conflicts of interest.

Abbreviations

The following abbreviations are used in this manuscript:

BH	Benjamini–Hochberg correction
CA19-9	Carbohydrate antigen 19-9
CAR	C-reactive protein-to-albumin ratio
CEA	Carcinoembryonic antigen
CRC	Colorectal cancer
dp-ucMGP	Dephosphorylated-uncarboxylated matrix Gla protein
ECW	Extracellular water
eGFR	Estimated glomerular filtration rate
FDR	False discovery rate
FFMI	Fat-free mass index
FMI	Fat mass index
HC3	Type 3 heteroscedasticity-consistent covariance estimator
ICW	Intracellular water
LVI	Lymphovascular invasion
MGP	Matrix Gla protein
PNI	Perineural invasion
pN	Pathological nodal category
pT	Pathological primary tumour category
TBW	Total body water
ypN	Pathological nodal category after neoadjuvant therapy
ypT	Pathological primary tumour category after neoadjuvant therapy

References

1. Bray, F.; Laversanne, M.; Sung, H.; Ferlay, J.; Siegel, R.L.; Soerjomataram, I.; Jemal, A. Global Cancer Statistics 2022: GLOBOCAN Estimates of Incidence and Mortality Worldwide for 36 Cancers in 185 Countries. *CA Cancer J. Clin.* **2024**, *74*, 229–263. https://doi.org/10.3322/caac.21834.
2. Guinney, J.; Dienstmann, R.; Wang, X.; De Reyniès, A.; Schlicker, A.; Soneson, C.; Marisa, L.; Roepman, P.; Nyamundanda, G.; Angelino, P.; et al. The Consensus Molecular Subtypes of Colorectal Cancer. *Nat. Med.* **2015**, *21*, 1350–1356. https://doi.org/10.1038/nm.3967.
3. Salem, M.E.; Weinberg, B.A.; Xiu, J.; El-Deiry, W.S.; Hwang, J.J.; Gatalica, Z.; Philip, P.A.; Shields, A.F.; Lenz, H.-J.; Marshall, J.L. Comparative Molecular Analyses of Left-Sided Colon, Right-Sided Colon, and Rectal Cancers. *Oncotarget* **2017**, *8*, 86356–86368. https://doi.org/10.18632/oncotarget.21169.
4. Duffy, M.J.; Lamerz, R.; Haglund, C.; Nicolini, A.; Kalousová, M.; Holubec, L.; Sturgeon, C. Tumor Markers in Colorectal Cancer, Gastric Cancer and Gastrointestinal Stromal Cancers: European Group on Tumor Markers 2014 Guidelines Update. *Int. J. Cancer* **2014**, *134*, 2513–2522. https://doi.org/10.1002/ijc.28384.
5. Luo, G.; Ducy, P.; McKee, M.D.; Pinero, G.J.; Loyer, E.; Behringer, R.R.; Karsenty, G. Spontaneous Calcification of Arteries and Cartilage in Mice Lacking Matrix GLA Protein. *Nature* **1997**, *386*, 78–81. https://doi.org/10.1038/386078a0.
6. Schurgers, L.J.; Cranenburg, E.C.M.; Vermeer, C. Matrix Gla-Protein: The Calcification Inhibitor in Need of Vitamin K. *Thromb. Haemost.* **2008**, *100*, 593–603. https://doi.org/10.1160/TH08-02-0087.
7. Cranenburg, E.; Koos, R.; Schurgers, L.; Magdeleyns, E.; Schoonbrood, T.; Landewé, R.; Brandenburg, V.; Bekers, O.; Vermeer, C. Characterisation and Potential Diagnostic Value of Circulating Matrix Gla Protein (MGP) Species. *Thromb. Haemost.* **2010**, *104*, 811–822. https://doi.org/10.1160/TH09-11-0786.
8. Dalmeijer, G.W.; Van Der Schouw, Y.T.; Magdeleyns, E.; Ahmed, N.; Vermeer, C.; Beulens, J.W.J. The Effect of Menaquinone-7 Supplementation on Circulating Species of Matrix Gla Protein. *Atherosclerosis* **2012**, *225*, 397–402. https://doi.org/10.1016/j.atherosclerosis.2012.09.019.
9. Griffin, T.P.; Islam, M.N.; Wall, D.; Ferguson, J.; Griffin, D.G.; Griffin, M.D.; O'Shea, P.M. Plasma Dephosphorylated-Uncarboxylated Matrix Gla-Protein (Dp-ucMGP): Reference Intervals in Caucasian Adults and Diabetic Kidney Disease Biomarker Potential. *Sci. Rep.* **2019**, *9*, 18452. https://doi.org/10.1038/s41598-019-54762-2.

10. Kremer, D.; Groothof, D.; Keyzer, C.A.; Eelderink, C.; Knobbe, T.J.; Post, A.; Van Londen, M.; Eisenga, M.F.; TransplantLines Investigators; Schurgers, L.J.; et al. Kidney Function-Dependence of Vitamin K-Status Parameters: Results from the TransplantLines Biobank and Cohort Studies. *Nutrients* **2021**, *13*, 3069. https://doi.org/10.3390/nu13093069.
11. Fan, C.-W.; Sheu, D.-L.; Fan, H.-A.; Hsu, K.-C.; Allen Chang, C.; Chan, E.-C. Down-Regulation of Matrix Gla Protein Messenger RNA in Human Colorectal Adenocarcinomas. *Cancer Lett.* **2001**, *165*, 63–69. https://doi.org/10.1016/S0304-3835(01)00416-5.
12. Caiado, H.; Conceição, N.; Tiago, D.; Marreiros, A.; Vicente, S.; Enriquez, J.L.; Vaz, A.M.; Antunes, A.; Guerreiro, H.; Caldeira, P.; et al. Evaluation of MGP Gene Expression in Colorectal Cancer. *Gene* **2020**, *723*, 144120. https://doi.org/10.1016/j.gene.2019.144120.
13. Li, X.; Wei, R.; Wang, M.; Ma, L.; Zhang, Z.; Chen, L.; Guo, Q.; Guo, S.; Zhu, S.; Zhang, S.; et al. MGP Promotes Colon Cancer Proliferation by Activating the NF-κB Pathway through Upregulation of the Calcium Signaling Pathway. *Mol. Ther. Oncolytics* **2020**, *17*, 371–383. https://doi.org/10.1016/j.omto.2020.04.005.
14. Huang, C.; Wang, M.; Wang, J.; Wu, D.; Gao, Y.; Huang, K.; Yao, X. Suppression MGP Inhibits Tumor Proliferation and Reverses Oxaliplatin Resistance in Colorectal Cancer. *Biochem. Pharmacol.* **2021**, *189*, 114390. https://doi.org/10.1016/j.bcp.2020.114390.
15. Rong, D.; Sun, G.; Zheng, Z.; Liu, L.; Chen, X.; Wu, F.; Gu, Y.; Dai, Y.; Zhong, W.; Hao, X.; et al. MGP Promotes $CD8^+$ T Cell Exhaustion by Activating the NF-κB Pathway Leading to Liver Metastasis of Colorectal Cancer. *Int. J. Biol. Sci.* **2022**, *18*, 2345–2361. https://doi.org/10.7150/ijbs.70137.
16. Perné, M.-G.; Sitar-Tăut, A.-V.; Orășan, O.H.; Negrean, V.; Vlad, C.V.; Alexescu, T.-G.; Milaciu, M.V.; Ciumărnean, L.; Togănel, R.D.; Petre, G.E.; et al. The Usefulness of Vitamin K-Dependent Proteins in the Diagnosis of Colorectal Carcinoma. *Int. J. Mol. Sci.* **2024**, *25*, 4997. https://doi.org/10.3390/ijms25094997.
17. GMON Software. Help Manual. Available online: https://www.gmon.eu/hlp_en (accessed on 19 November 2026).
18. Amin, M.B.; Edge, S.B.; Greene, F.L.; Byrd, D.R.; Brookland, R.K.; Washington, M.K.; Gershenwald, J.E.; Compton, C.C.; Hess, K.R.; Sullivan, D.C.; et al. (Eds.) *AJCC Cancer Staging Manual*, 8th ed.; Springer: Cham, Switzerland, 2017; ISBN 978-3-319-40617-6.
19. Schurgers, L.J.; Barreto, D.V.; Barreto, F.C.; Liabeuf, S.; Renard, C.; Magdeleyns, E.J.; Vermeer, C.; Choukroun, G.; Massy, Z.A. The Circulating Inactive Form of Matrix Gla Protein Is a Surrogate Marker for Vascular Calcification in Chronic Kidney Disease: A Preliminary Report. *Clin. J. Am. Soc. Nephrol.* **2010**, *5*, 568–575. https://doi.org/10.2215/CJN.07081009.
20. Puzantian, H.; Akers, S.R.; Oldland, G.; Javaid, K.; Miller, R.; Ge, Y.; Ansari, B.; Lee, J.; Suri, A.; Hasmath, Z.; et al. Circulating Dephospho-Uncarboxylated Matrix Gla-Protein Is Associated With Kidney Dysfunction and Arterial Stiffness. *Am. J. Hypertens.* **2018**, *31*, 988–994. https://doi.org/10.1093/ajh/hpy079.
21. Wei, F.-F.; Trenson, S.; Thijs, L.; Huang, Q.-F.; Zhang, Z.-Y.; Yang, W.-Y.; Moliterno, P.; Allegaert, K.; Boggia, J.; Janssens, S.; et al. Desphospho-Uncarboxylated Matrix Gla Protein Is a Novel Circulating Biomarker Predicting Deterioration of Renal Function in the General Population. *Nephrol. Dial. Transplant.* **2018**, *33*, 1122–1128. https://doi.org/10.1093/ndt/gfx258.
22. Brnic, D.; Martinovic, D.; Zivkovic, P.M.; Tokic, D.; Vilovic, M.; Rusic, D.; Hadjina, I.T.; Libers, C.; Glumac, S.; Supe-Domic, D.; et al. Inactive Matrix Gla Protein Is Elevated in Patients with Inflammatory Bowel Disease. *World J. Gastroenterol.* **2020**, *26*, 4866–4877. https://doi.org/10.3748/wjg.v26.i32.4866.
23. Vieujean, S.; Gillard, R.; Delanaye, P.; Seidel, L.; Bequet, E.; Salée, C.; Meuwis, M.-A.; Massot, C.; Pierre, N.; Meunier, P.; et al. Matrix Gla Protein, a Potential Marker of Tissue Remodelling and Physiological Ageing of the Gut in Crohn's Disease. *Scand. J. Gastroenterol.* **2024**, *59*, 296–303. https://doi.org/10.1080/00365521.2023.2286913.
24. Šantić, R.; Pavlović, N.; Kumrić, M.; Vilović, M.; Božić, J. Pathophysiological Links Between Inflammatory Bowel Disease and Cardiovascular Disease: The Role of Dysbiosis and Emerging Biomarkers. *Biomedicines* **2025**, *13*, 1864. https://doi.org/10.3390/biomedicines13081864.
25. Jespersen, T.; Møllehave, L.T.; Thuesen, B.H.; Skaaby, T.; Rossing, P.; Toft, U.; Jørgensen, N.R.; Corfixen, B.L.; Jakobsen, J.; Frimodt-Møller, M.; et al. Uncarboxylated Matrix Gla-Protein: A Biomarker of Vitamin K Status and Cardiovascular Risk. *Clin. Biochem.* **2020**, *83*, 49–56. https://doi.org/10.1016/j.clinbiochem.2020.05.005.
26. Lauridsen, J.A.; Leth-Møller, K.B.; Møllehave, L.T.; Kårhus, L.L.; Dantoft, T.M.; Kofoed, K.F.; Linneberg, A. Investigating the Associations between Uncarboxylated Matrix Gla Protein as a Proxy for Vitamin K Status and Cardiovascular Disease Risk Factors in a General Adult Population. *Eur. J. Nutr.* **2025**, *64*, 17. https://doi.org/10.1007/s00394-024-03532-6.
27. Vidula, M.K.; Akers, S.; Ansari, B.A.; Kim, J.; Kumar, A.A.; Tamvada, D.; Satija, V.; Mohan-Rao Vanjarapu, J.; Jehangir, Q.; Magro, C.; et al. Increased Dephospho-Uncarboxylated Matrix Gla-Protein Is Associated With Lower Axial Skeletal Muscle Mass in Patients With Hypertension. *Am. J. Hypertens.* **2022**, *35*, 393–396. https://doi.org/10.1093/ajh/hpab190.

Disclaimer/Publisher's Note: The statements, opinions and data contained in all publications are solely those of the individual author(s) and contributor(s) and not of MDPI and/or the editor(s). MDPI and/or the editor(s) disclaim responsibility for any injury to people or property resulting from any ideas, methods, instructions or products referred to in the content.

https://doi.org/10.3390/medsci14080808